Journal of
Composites Science

MDPI

Article

Green Synthesis of Selenium Nanoparticles Using *Cleistocalyx operculatus* Leaf Extract and Their Acute Oral Toxicity Study

Tri Thien Vu [1], Phuong Thi Mai Nguyen [2,3], Ngan Hanh Pham [4], Thanh Huu Le [1], Tran Hung Nguyen [1,*], Dinh Trung Do [5] and Duong Duc La [1,*]

[1] Institute of Chemistry and Materials, Nghia Do, Cau Giay, Hanoi 100000, Vietnam
[2] Institute of Graduate University of Science and Technology, Vietnam Academy of Science and Technology, 18 Hoang Quoc Viet Road, Cau Giay, Hanoi 100000, Vietnam
[3] Institute of Biotechnology, Vietnam Academy of Science and Technology, 18 Hoang Quoc Viet Road, Cau Giay, Hanoi 100000, Vietnam
[4] Faculty of Chemistry, Hanoi National University of Education, 136 Xuan Thuy, Dich Vong Hau, Cau Giay, Hanoi 100000, Vietnam
[5] Institute of Tropical Durability, Joint Vietnam-Russia Tropical Science and Technology Research Center, Nghia Do, Hanoi 100000, Vietnam
* Correspondence: nguyentranhung28@gmail.com (T.H.N.); duc.duong.la@gmail.com (D.D.L.)

Abstract: Green synthesis has recently attracted extensive attention from scientists all over the world for the production of metal nanoparticles. Selenium nanoparticles (Se NPs) have been demonstrated as a suitable supplement nutrient for the replacement of selenium ions in terms of safety and efficiency. This work presented a friendly and facile approach to synthesize the Se NPs using polyphenols content in the *Cleistocalyx operculatus* (CO) leaves extract. The synthesizing conditions were optimized to obtain the Se NPs with uniform distribution and shape. The prepared Se NPs were well-characterized using scanning electron microscopy, X-ray diffraction, energy diffractive spectroscopy, and Fourier-transform infrared spectroscopy. The resultant Se NPs were in spherical shape with the particle size in a range from 50–200 nm. The antimicrobial properties of Se NPs were investigated against *Echerichia coli* and *Staphylococcus aureus*, which showed reasonable activity. The acute oral toxicity of Se NPs in mice was also studied. The result indicated that Se NPs exhibited lower toxicity than that of SeO_2 with the lethal concentration (50% death of mice) of 7.75 mg kg^{-1}.

Keywords: selenium nanoparticles; *Cleistocalyx operculatus*; green synthesis; acute toxicity; anti-bacterial

Citation: Vu, T.T.; Nguyen, P.T.M.; Pham, N.H.; Le, T.H.; Nguyen, T.H.; Do, D.T.; La, D.D. Green Synthesis of Selenium Nanoparticles Using *Cleistocalyx operculatus* Leaf Extract and Their Acute Oral Toxicity Study. *J. Compos. Sci.* **2022**, *6*, 307. https://doi.org/10.3390/jcs6100307

Academic Editor: Huirong Le

Received: 15 September 2022
Accepted: 8 October 2022
Published: 12 October 2022

1. Introduction

The last few decades have witnessed a rapid growth in the development and research of nanomaterials globally because of their unique properties in many fields of application [1,2]. Many approaches could be employed to synthesize metallic nanoparticles, which consist of chemical, physical, and biological approaches. While the physical methods are time-consuming processes requiring a lot of energy as well as occupying spaces, the chemical methods commonly use toxic-reducing agents for the synthesis of nanoparticles [3,4]. Thus, the chemical and physical approaches are considered not suitable for the production of nanoparticles on a large scale [5]. Because of the aforementioned issues, the biological methods for nanoparticles synthesis are preferred for nanomaterials fabrication. The biological approaches utilize fungi, bacteria, algae, and plant extracts as green agents for reducing metal ions into their metallic form with sizes ranging from 1–100 nm [6–9].

Many plant and plant parts (green tea leaf, *Ficus carica* dried fruit, *Avicennia marina* flower . . .) have been successfully employed to fabricate nanoparticles such as silver, zero-valent iron nanoparticles, copper, zinc oxide, and gold [10–13]. The use of reductants from the plant extracts could significantly reduce production cost, environmental issues, and improve the quality and stability of the resultant nanoparticles. It is of note that

the extract from each plant has unique chemical and biological properties as well as reducing activity depending on the polyphenol contents in the extract. Moreover, the regional conditions (weather, soils, and water) where the plant grows will decide the quality and reducing capability of the plant extracts. Thanks to the tropical weather and the diversity of plants, Vietnamese scientists have recently focused on the green synthesis of nanoparticles using plant extracts. One of the most promising plant extracts that could be employed as a green reducing agent is the extract from *Cleistocalyx operculatus* (CO) leaves. This plant is a well-known native plant for medicine and beverages, containing a high proportion of polyphenols as the main reducing component, which could reduce metal ions to nanoparticles. Several works have been undertaken to fabricate nanoparticles using the CO extract. For example, Nguyen et al. successfully utilized the CO extract as a green reductant to synthesize zero-valent iron nanoparticles (nZVIs) [10]. The prepared nZVIs showed remarkable degrading efficiency toward Rhodamine B with a removal percentage of up to 95% in 30 min. Interestingly, the resultant nZVIs exhibited high stability, thanks to a thin organic coating formed by polysaccharides in the CO extract.

Selenium is one of the trace minerals that is evident to be crucial for many mammalian creatures and human body [14,15]. It could incorporate with the proteins to appropriately function in the immune systems and adjusting the function of the thyroid gland; as a result, avoid cellular damage [16]. Additionally, with reasonable antibacterial property, selenium has been studied as an anti-carcinogenic substance for many types of cancers [17,18]. However, selenium could have many side effects if an over-dose of this trace mineral is administered in the human body, even causing death for people. Thus, finding a suitable form of Selenium (Se) to optimize the advantages of Selenium usage, while avoiding the adverse effects of an overdose of this trace element become urgent [19]. To meet this urgent demand, many scientists worldwide have recently paid close attention to replacing the Se element with the Se particles in nanoscale. Selenium nanoparticles (Se NPs) have many advantages such as low toxicity, biocompatibility, unique therapeutic properties, and bioavailability, which could be utilized in many biomedical and physiological applications [20,21]. Se NPs could be employed as chemopreventive and anti-cancer substances, antimicrobial agents, in sensing, in electronic devices, catalysis, imaging, and photovoltaic applications [22–27]. Se NPs could be obtained from various pathways including, but not limited to, chemical and electrochemical reactions, laser ablation, solution plasma method, and green synthesis using biological agents [28–34]. Among these, Se NPs obtained from green synthesis using plant extracts as reducing agent demonstrated to be economic, less toxic, and have large-scale production capability [35–38]. However, to the best of our knowledge, no work has been undertaken to employ the high content of polyphenol extract in the CO leaf as a reducing agent for the synthesis of Se NPs, especially with reference to the acute oral toxicity of the resultant Se NPs.

Herein, Se NPs are successfully fabricated using the CO extract as a green reductant. The resultant Se NPs are well-characterized using scanning electron microscopy, UV-vis spectroscopy, transmittance electron microscopy, X-ray diffraction, FTIR spectroscopy, and Energy dispersive spectroscopy. The acute oral toxicity of Se NPs in mice is also studied and discussed.

2. Materials and Methods

2.1. Materials

C. operculatus collected in Hanoi, Vietnam was washed, dried at 105 degrees and ground to a fine powder. We heated 5 g of dry powder in 96% ethanol at 60 degrees for 2 h. Next, the extract was filtered and analyzed for total polyphenol and flavonoid content. The total content of polyphenols and flavonoids was determined to be 12.4 mg/mL, 0.63 mg/mL, respectively. *C. operculatus* leaf extract was diluted 5 times with distilled water to be used for synthesis.

Selenium dioxide (SeO_2, 99.99%) was received from Sigma-Aldrich, St. Louis, MO, USA. The H_2SeO_3 solution was prepared by dilution of SeO_2 in double-distilled water with a concentration of 3 mM. All chemicals were used as received without any additional purification.

2.2. Green Synthesis of Selenium Nanoparticles

SeNPs were synthesized by slowly adding H_2SeO_3 solution to *C. operculatus* leaf extract, which had been heated to a temperature of 40 degrees, according to the ratio of volume of extract/H_2SeO_3 in turn 1:1; 2:1; 3:1; 4:1. The mixture was magnetically stirred for 2 h at 40 degrees. The selenium nanoparticle dispersion solution was stored at 5 degrees and used for further analysis.

2.3. Characterization of Selenium Nanoparticles

SeNPs were characterized by UV–Visible spectroscopy (Hitachi-UH4150, Tokyo, Japan). The morphology of the Se NPs was observed via field emission scanning electron microscopy (SEM-EDX, Hitachi S-4600). The detailed structure was analyzed via transmission electron microscopy (TEM, JEM-2100F, JEOL) and high-resolution transmission electron microscopy (TEM, JEOL JEM 1010). The elemental analysis of the prepared Se NPs was studied using energy-dispersive X-ray spectroscopy (Hitachi S-4600). The crystal structure of Se NPs was obtained on an X-ray diffractometer (XRD, X'Pert PRO PANalytical) with Cu Kα (λ = 1.5418 Å) radiation operating at 45 kV and 200 mA. The XRD patterns were acquired in the range of 20–70° with a step size of 0.01° and a scan speed of 1 min^{-1}. Functional groups were analyzed by FT-IR (Brucker-Tensor II). The IR spectrum was recorded in middle region wavenumber of 4000–400 cm^{-1} at a resolution of 4.0 cm^{-1}.

2.4. Acute Toxicity

Forty-eight healthy BALB/c white mice, with a weight of about 22–26 g, regardless of breed, were raised in the animal house under standard conditions of temperature and light, then they were divided into eight lots (six rats/lot) and starved for 16 h before drinking the study sample. Se NPs dispersed in 0.9% pathogen-free NaCl were administered orally at different doses. The animals were observed for survival and clinical signs of toxicity on the dosing day and then daily for 14 days. The cumulative mortality rate within 72 h of treatment was used to calculate the mean fatal dose (LD50).

2.5. Anti-Bacterial Activity

The standard well diffusion method was employed to study the antimicrobial property of Se-NPs against *Echerichia coli* and *Staphylococcus aureus*. We fabricated 6 mm wells on Muller–Hilton agar plates using gel puncture. Amounts of 25, 50, 75 and 100 µL of the Se NPs with a concentration of 300 ppm and Streptomycine (0.1 g/mL) as the control were introduced into the wells using a micropipette. The experiments were replicated three times. The different levels of the inhibition zones were recorded after incubation at 37 °C for 24 h. The diameters of the inhibition zones around each well were determined.

3. Results and Discussion

3.1. Effect of the Stirring Methods

During the reduction of Se ions to Se NPs by the CO extract, the stirring methods have a great effect on the morphologies of resultant Se NPs. Figure 1 shows the morphologies of the Se NPs synthesized using the CO extract with the assistance of probe sonicating, bath sonicating, and magnetic stirring. It can be clearly seen that Se NPs obtained in the probe and bath sonicating methods reveal aggregate form with undefined morphologies. These might be due to the strong stirring energy from the sonicating method, which could break the structure of newly formed Se NPs, leading to aggregation and undefined morphology. When magnetic stirring was used for the reducing process of Se ions by the CO extract, the resultant Se NPs exhibited relatively well-defined spherical shape with partial aggregation, which is explained by the polysaccharide contents in the CO extract. Thus, the magnetic

stirrer is selected as the optimal stirring method to assist the synthesis of Se NPs using the CO extract [39,40].

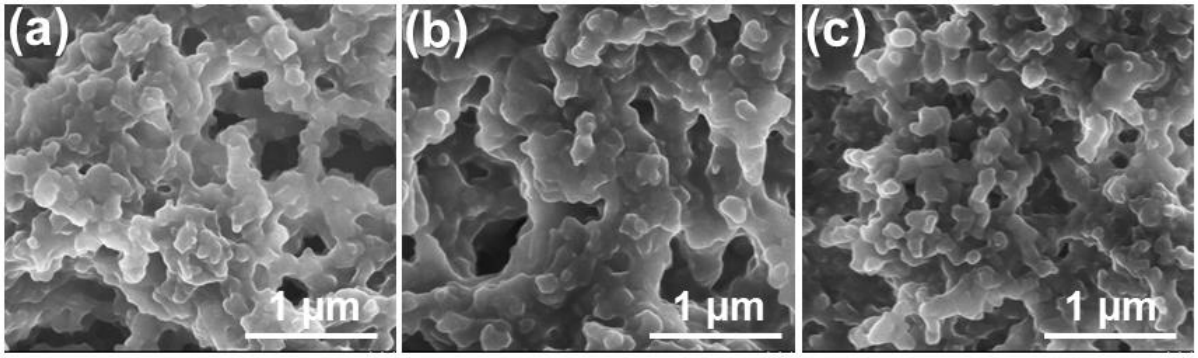

Figure 1. SEM images of Se NPs synthesized by the CO extract with the assistance of (**a**) probe sonicating, (**b**) bath sonicating, and (**c**) magnetic stirring with Se^{4+}/CO volume ratio of 1/1.

3.2. Effect of the Se^{4+}/CO Volume Ratios

Figure 2 shows the morphologies of the Se NPs synthesized from Se^{4+} precursor using the CO extract with various Se^{4+}/CO volume ratios. With the Se^{4+}/CO volume ratio of 1/1, Se nanoparticles are in irregular and undefined shapes. The round and defined spherical shapes are clearly observed with relative uniformity in size distribution at the Se^{4+}/CO volume ratio of 1/2. Further increases in the Se^{4+}/CO volume ratios witness the aggregation form of the Se NPs, which might be due to the presence of high polysaccharide content in the CO extract that could bind Se NPs particle together. Thus, the Se^{4+}/CO volume ratio of 1/1 was selected as an optimal CO extract's content for the synthesis of Se NPs.

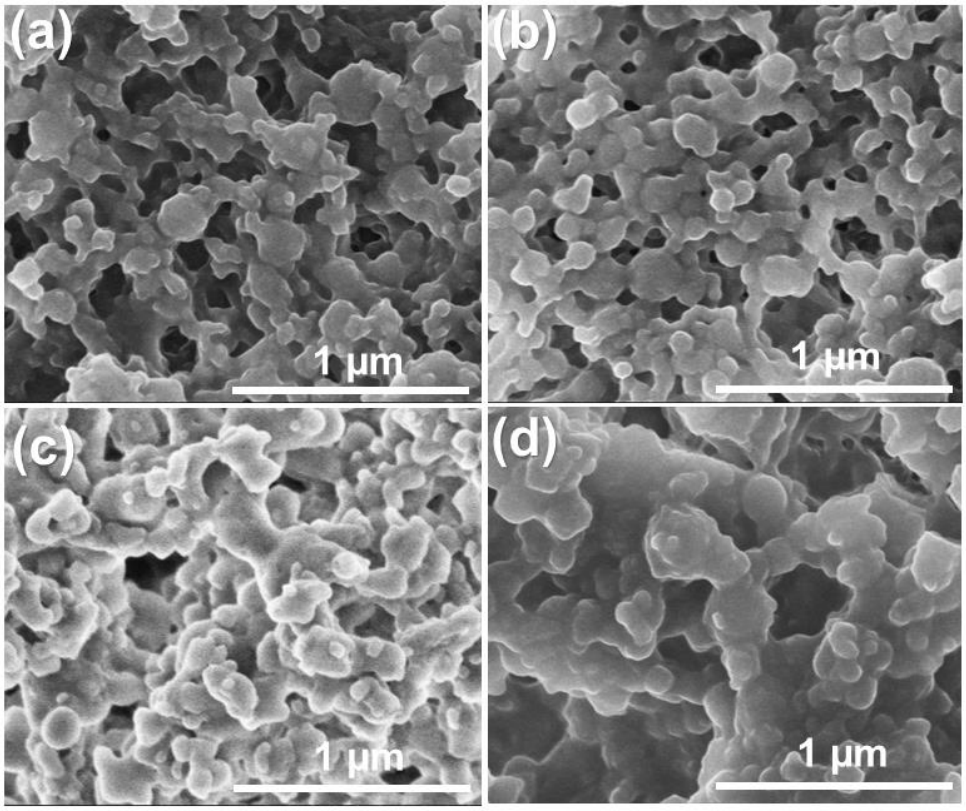

Figure 2. SEM images of Se NPs prepared from the CO extract under magnetic stirring condition with the Se^{4+}/CO volume ratio of (**a**) 1/1, (**b**) 1/2, (**c**) 1/3, and (**d**) 1/4.

3.3. Characterization of Se NPs

It has been well evident from previous works that the polyphenols content in the leaf extract could reduce Se^{4+} ions to form metallic Se NPs [36,41,42]. With a polyphenols contents of approximately 13%, the CO extract could be utilized as an effective reducing agent for the green synthesis of metallic nanoparticles [4,10]. In this work, the CO extract was employed as a reductant to synthesise Se NPs from Se^{4+} precursor; the formation of Se NPs was initially observed using UV-vis spectroscopy. Figure 3 shows the UV-vis spectrum and optical images of the resultant Se NPs. When the diluted CO extract, in light yellow colour, reacted with the Se^{4+} precursor, in transparent colour, a light red solution was obtained, which is demonstrated to be a typical colour of the metallic Se NPs [43]. This colour change was observed only after 30 min and completed after 2 h of reaction time. The red colour of the resultant solution is ascribed to the surface plasmon vibration in excitation state from SE NPs [44]. It has been well known in the literature that the UV-vis spectrum of Se^{4+} ions shows no absorption peak, indicating no surface plasmon vibration effect occurs in this state. Intriguingly, the UV-vis spectrum of Se NPs in Figure 3 exhibits a high-intensity absorption peak at 302 nm. This absorption band is ascribed to the surface plasmon vibration in excitation state of Se NPs [45]. This result primarily assures us that the polyphenols content in the CO extract successfully reduced the Se precursor to form metallic Se NPs.

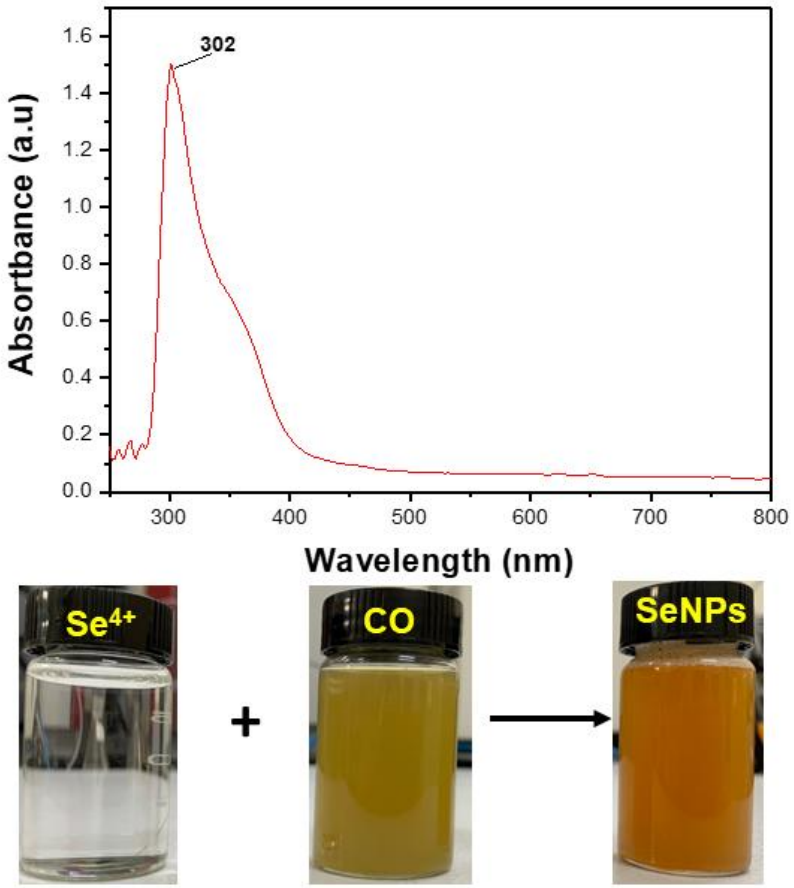

Figure 3. Optical images of Se^{4+} precursor, the CO extract, Se NPs, and UV-spectrum of Se NPs prepared with the Se^{4+}/CO volume ratio of 1/2.

The morphologies and size distribution of the Se NPs obtained from Se^{4+} precursor using the CO extract with the Se^{4+}/CO volume ratio of 1/2 were studied using SEM and TEM images and the result is shown in Figure 4. It is obvious in the low SEM resolution image that the resultant Se NPs are round in shape with a uniform distribution (Figure 4a). The high SEM resolution image exhibits the spherical morphology of Se NP with a diameter

ranging from 50–200 nm (Figure 4b). This particle size and shape were further confirmed by the TEM images as shown in Figure 4c,d. The SEM and TEM images also show the presence of the thin coating on the surface of Se NPs, which is ascribed to the polysaccharide compounds in the CO extract [10].

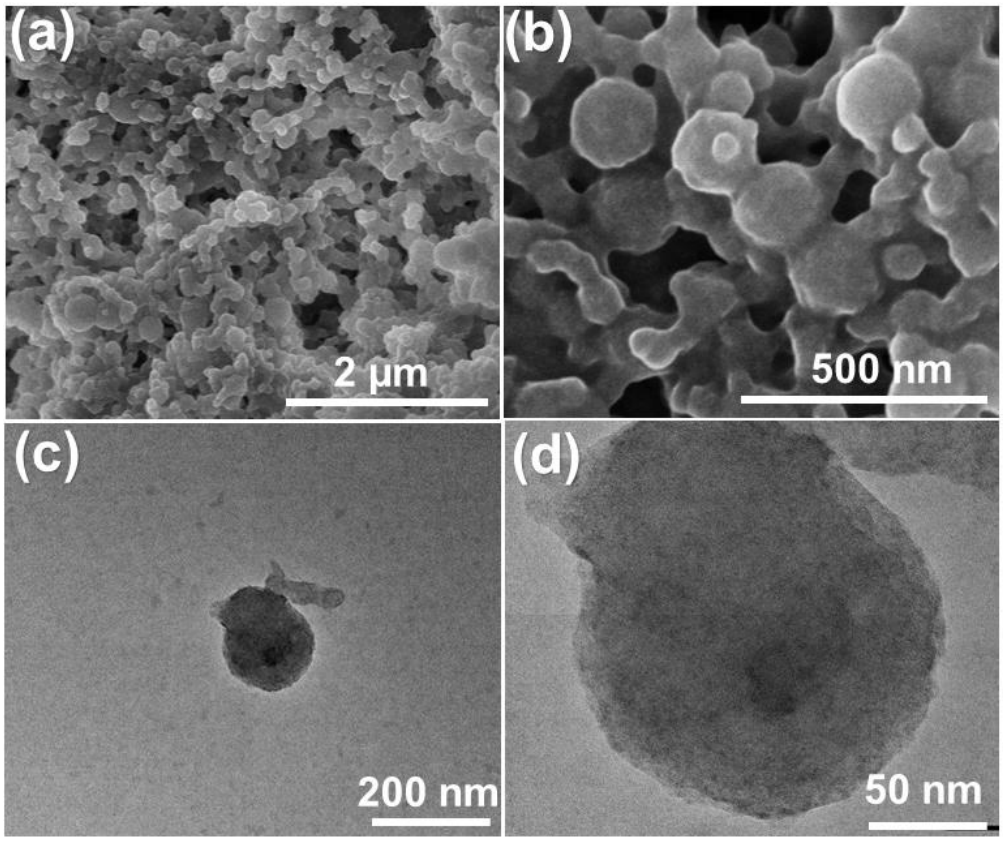

Figure 4. SEM (**a**,**b**) and TEM (**c**,**d**) images of the Se NPs prepared with the Se^{4+}/CO volume ratio of 1/2.

The elemental composition and distribution in Se NPs was investigated by EDS spectrum and EDS mapping as shown in Figure 5. The characteristic peaks of the SeLα and SeKβ from Se NPs were observed at 1.4 and 11.2 keV, respectively, in the EDS spectrum [16]. The spectrum also shows high intensity peaks of the C and O presence in the Se NPs materials. These elements could belong to the organic coating on the Se NPs' surface, which further confirms the presence of polysaccharide compounds in the CO extract. This thin coating film could protect Se NPs from oxidation. The EDS mapping of the Se NPs also assures the presence of the Se, C, and O in the final product.

The appearance and crystallinity of the Se NPs in the sample were further confirmed using X-ray diffraction analysis. The XRD pattern of the Se NPs prepared with the Se^{4+}/CO volume ratio of 1/2 is shown in Figure 6. The diffraction peaks at around 20 and 30° in the XRD pattern are assigned to the (100) and (101) planes, respectively, of metallic Se nanoparticles with trigonal phase containing lattice constants in structure: a = 4.366 Å and c = 4.956 Å (JCPDS file no. 06-362) [32,46]. The other peaks present in the XRD spectrum might be attributed to the diffraction peaks of the selenium oxide, which is partially oxidized from the presence of oxygen in the media reaction.

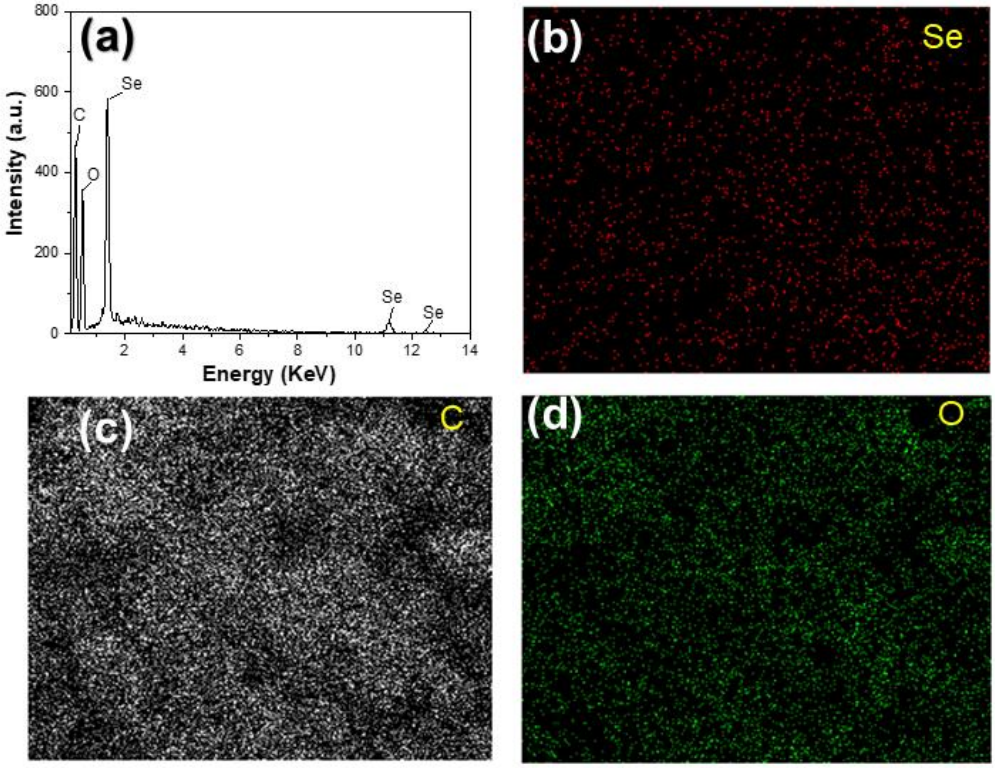

Figure 5. (**a**) EDS spectrum and EDX mapping (**b**–**d**) of the Se NPs prepared with the Se^{4+}/CO volume ratio of 1/2.

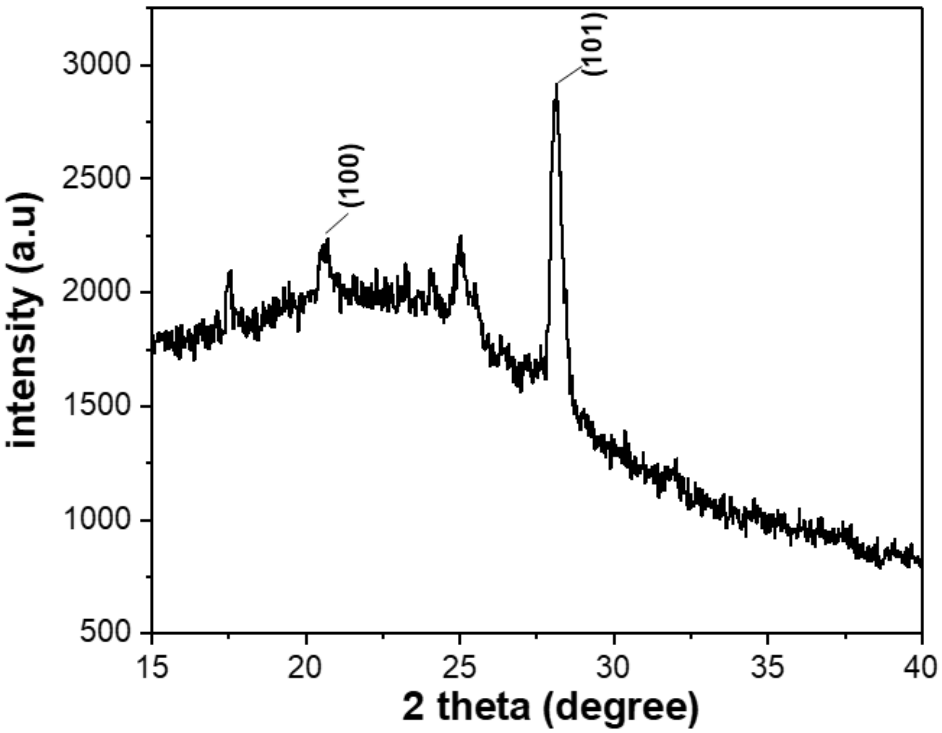

Figure 6. XRD pattern of the Se NPs prepared with the Se^{4+}/CO volume ratio of 1/2.

The chemical bonding nature in the Se NPs product was investigated using FTIR spectroscopy and the result is shown in Figure 7. The broad absorption band ranging from 3200–3600 cm^{-1} in the FTIR spectrum belong to the O-H bonding of moisture, alcohols, and phenols groups in the extract [10,47,48]. The characteristic vibration appearing at 2930 cm^{-1}

is assigned to the C-H stretching bonds of alkynes. The C=O stretching group in the cetone and aldehyde groups is also observed at 1687 cm^{-1} in the FTIR spectrum. The strong vibration peaks at 1607 cm^{-1} and 1430 cm^{-1} are attributed to the N-O asymmetric bonding in nitro compounds and C-C bonding in ring of aromatics, respectively. The strong absorption peak at 1350 cm^{-1} is assigned to the C-H stretching in alkanes. Several vibration bands at 1100 and 1048 cm^{-1} are attributed to the C-N bending of the amines [35]. The O-H group in the carboxylic acids is also evident at the vibration band of 942 cm^{-1}. The characteristic FTIR peak at 765 cm^{-1} is ascribed to the bending of C-H in alkyl halides. This result demonstrates that the prepared Se NPs' surfaces were successfully covered by various functional groups, which are responsible for the reduction as well as stabilization of the resultant Se NPs. The organic compounds in the extract have been demonstrated to be stabilizing agents for the metal nanoparticles [29]. However, further study on the active molecules responsible for the synthesis as well as the protection of the Se NPs is needed.

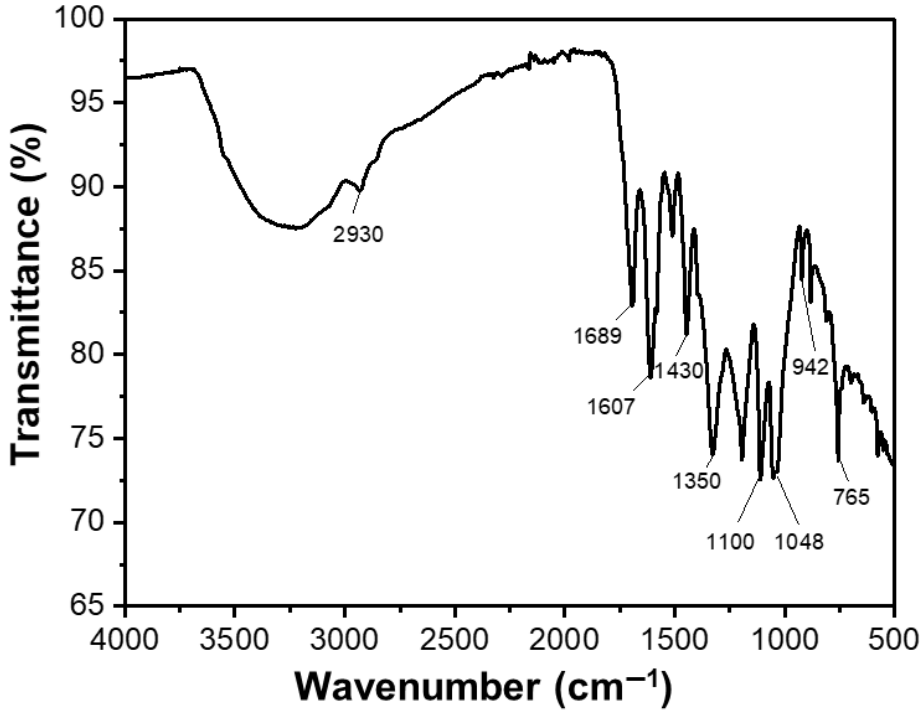

Figure 7. FTIR spectrum of the Se NPs prepared with the Se^{4+}/CO volume ratio of 1/2.

3.4. Antimicrobial Activity

Figure 8 shows the antimicrobial activity of the Se NPs prepared with the Se^{4+}/CO volume ratio of 1/2 with the assistance of magnetic stirring against *Echerichia coli* and *Staphylococcus aureus* at various doses of 25, 50, 75, and 100 µL. The inhibition zones of the Se NPs for *E. coli* were calculated to be 12, 13, 13, and 15 mm at the dosage of 25, 50, 75, and 100 µL, respectively, with a Se NPs' concentration of 300 ppm, which is relatively high bioactivity considering the low concentration of Se NPs. For the *S. aureus*, the Se NPs show inhibition zones of around 10 mm for all the dosages. This result indicates that the Se NPs prepared by the CO extract reveals effective microbial activity against *E. coli* bacteria.

3.5. Acute Oral Toxicity and Lethal Concentration (LC50) of Se NPs

The toxicity and ecotoxicology of metal nanoparticles are commonly investigated using the lethal concentration (LC50) and acute toxicity protocols. The lethal concentration is the dosage of nanoparticles that causes the death of 50% of test animals in a certain period of time. This factor is important to evaluate the safety of nanoparticles employed in animals and the human body in terms of biological and ecological aspects. This study investigated the effect of Se NPs prepared by the CO extract with the Se^{4+}/CO volume ratio of 1/2 on the

acute toxicity and response of mice during 72 h of administration. Figure 9 exhibits the optical images of mice administrated with various doses of 300 ppm Se NPs. It is obvious from the result that the activity and food consumption of mice with normal responses to surrounding environments were observed at the Se NPs' dosage of <4.5 mg kg^{-1} (data not shown), which is the same as the control mice. The food consumption of mice significantly decreased and the response to the surroundings weakened with a Se NPs' dose of >4.5 mg kg^{-1}. The lethal concentration (50 % of dead mice) of the Se NPs for mice was determined to be approximately 7.75 mg kg^{-1}. Previous work revealed that the lethal concentration of SeO_2 for mice was calculated to be 2.5 mg kg^{-1} [49]. This means that the lethal concentration of the Se NPs is around 3 times higher than that of SeO_2. The result confirms that the Se NPs synthesized by the CO extract with less solubility, safe chemical form and oxidative state could minimize the acute oral toxicity compared to the Se ions form.

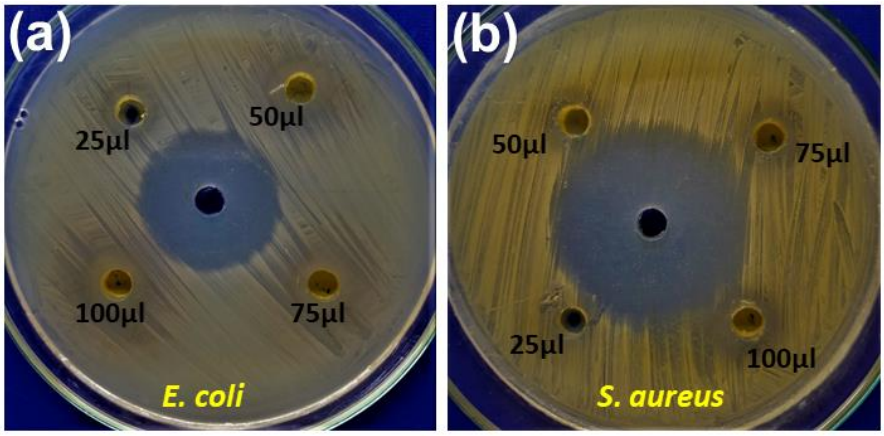

Figure 8. Bioactivity of the Se prepared with the Se^{4+}/CO volume ratio of 1/2 against (**a**) *E. coli* and (**b**) *S. aureus* at the Se NPs various doses of 25, 50, 75, and 100 µL (concentration of 300 ppm).

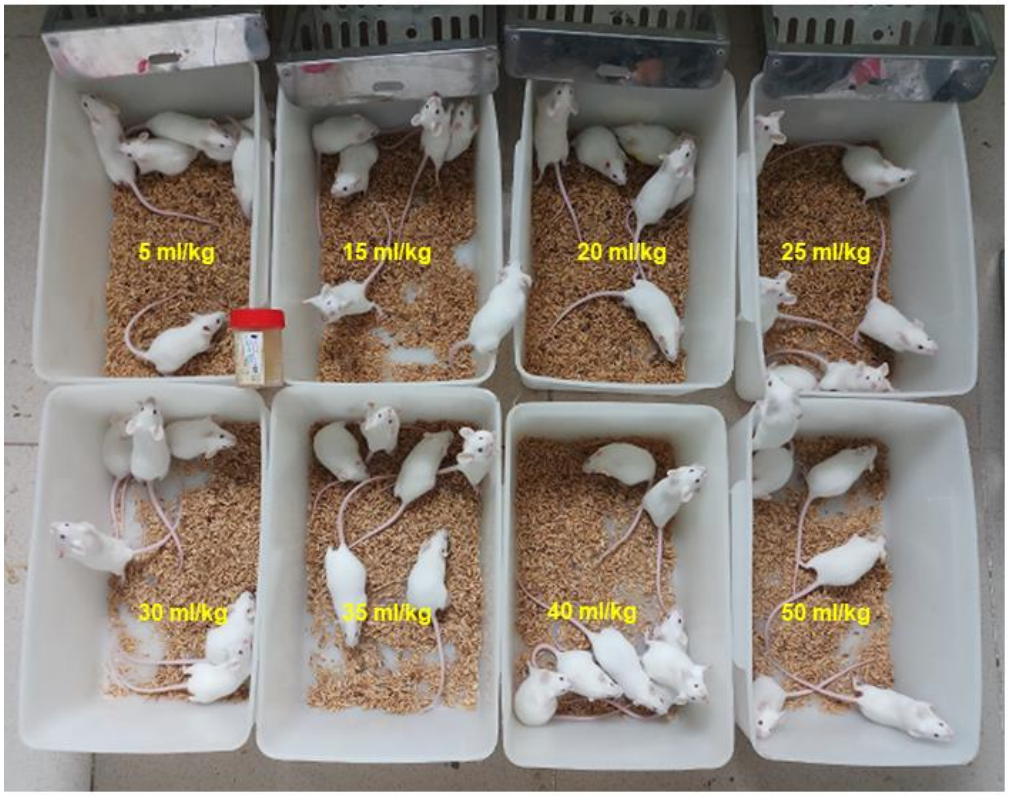

Figure 9. Optical images of mice administered with various doses of 300 ppm Se NPs.

4. Conclusions

In short, the selenium nanoparticles have been successfully synthesized using the polyphenols content in the CO extract as reductant. The Se NPs prepared with the Se^{4+}/CO volume ratio of 1/2 and the assistance of magnetic stirring were of spherical shape with a diameter in the range of 50–200 nm. The resultant Se NPs were demonstrated to be stabilized by a thin organic coating from the polysaccharide content in the CO extract. The prepared Se NPs revealed a reasonable antimicrobial activity against *Echerichia coli* and *Staphylococcus aureus* with inhibition zones of 15 mm at the dose of 100 µL with Se NPs' concentration of 300 ppm. In comparison to the SeO_2, the Se NPs prepared using the CO extract exhibited lower acute oral toxicity with the lethal concentration (50% death of animals) of the Se NPs for mice determined to be approximately 7.75 mg kg^{-1}, which is about 3 times lower than that of SeO_2. The mice revealed normal food consumption and activity after the uptake of Se NPs during the test time, which indicates that Se NPs prepared by the CO extract is safe for humans and animals. For this reason, Se NPs could be considered as a promising supplement nutrient to replace Se in ion form for humans and animals.

Author Contributions: Conceptualization—T.H.N., D.D.L. and D.T.D.; methodology—T.T.V., D.D.L. and N.H.P.; software—T.H.L.; investigation—T.T.V., D.D.L., D.T.D. and N.H.P.; data curation—T.T.V. and T.H.L.; writing—original draft—T.T.V. and D.D.L.; writing—reviewing scientific contents and editing—T.H.N., D.D.L., P.T.M.N. and D.T.D. All authors have read and agreed to the published version of the manuscript.

Funding: This work was financially funded by the e-ASIA JRP (Project No. NĐT.74.e-ASIA/19).

Institutional Review Board Statement: Not applicable.

Informed Consent Statement: Not applicable.

Data Availability Statement: Not applicable.

Acknowledgments: The authors thank staffs at Institute of Chemistry and Materials for the support in characterizing and analysis. We also thank the Institute for all facilities we used to carry out the work.

Conflicts of Interest: The authors declare that no conflict of interest exist in the submission of this manuscript.

References

1. Baer, D.R.; Amonette, J.E.; Engelhard, M.; Gaspar, D.; Karakoti, A.; Kuchibhatla, S.; Nachimuthu, P.; Nurmi, J.T.; Qiang, Y.; Sarathy, V.; et al. Characterization challenges for nanomaterials. *Surf. Interface Anal.* **2008**, *40*, 529–537. [CrossRef]
2. Lines, M. Nanomaterials for practical functional uses. *J. Alloys Compd.* **2008**, *449*, 242–245. [CrossRef]
3. Tarasenko, N.; Butsen, A.; Nevar, E.; Savastenko, N. Synthesis of nanosized particles during laser ablation of gold in water. *Appl. Surf. Sci.* **2006**, *252*, 4439–4444. [CrossRef]
4. Jadoun, S.; Arif, R.; Jangid, N.K.; Meena, R.K. Green synthesis of nanoparticles using plant extracts: A review. *Environ. Chem. Lett.* **2020**, *19*, 355–374. [CrossRef]
5. Pal, G.; Rai, P.; Pandey, A. Green Synthesis of Nanoparticles: A Greener Approach for a Cleaner Future. In *Green Synthesis, Characterization and Applications of Nanoparticles*; Elsevier: Amsterdam, The Netherlands, 2019; pp. 1–26. [CrossRef]
6. Ayano, H.; Miyake, M.; Terasawa, K.; Kuroda, M.; Soda, S.; Sakaguchi, T.; Ike, M. Isolation of a selenite-reducing and cadmium-resistant bacterium Pseudomonas sp. strain RB for microbial synthesis of CdSe nanoparticles. *J. Biosci. Bioeng.* **2014**, *117*, 576–581. [CrossRef] [PubMed]
7. Yadav, A.; Kon, K.; Kratošová, G.; Durán, N.; Ingle, A.P.; Rai, M. Fungi as an efficient mycosystem for the synthesis of metal nanoparticles: Progress and key aspects of research. *Biotechnol. Lett.* **2015**, *37*, 2099–2120. [CrossRef]
8. Aziz, N.; Faraz, M.; Pandey, R.; Shakir, M.; Fatma, T.; Varma, A.; Barman, I.; Prasad, R. Facile Algae-Derived Route to Biogenic Silver Nanoparticles: Synthesis, Antibacterial, and Photocatalytic Properties. *Langmuir* **2015**, *31*, 11605–11612. [CrossRef]
9. Duan, H.; Wang, D.; Li, Y. Green chemistry for nanoparticle synthesis. *Chem. Soc. Rev.* **2015**, *44*, 5778–5792. [CrossRef]
10. Le, N.T.; Dang, T.-D.; Binh, K.H.; Nguyen, T.M.; Xuan, T.N.; La, D.D.; Nadda, A.K.; Chang, S.W.; Nguyen, D.D. Green synthesis of highly stable zero-valent iron nanoparticles for organic dye treatment using *Cleistocalyx operculatus* leaf extract. *Sustain. Chem. Pharm.* **2022**, *25*, 100598. [CrossRef]

11. Onitsuka, S.; Hamada, T.; Okamura, H. Preparation of antimicrobial gold and silver nanoparticles from tea leaf extracts. *Coll. Surf. B Biointerfaces* **2018**, *173*, 242–248. [CrossRef]
12. Alamdari, S.; Ghamsari, M.S.; Lee, C.; Han, W.; Park, H.-H.; Tafreshi, M.J.; Afarideh, H.; Ara, M.H.M. Preparation and Characterization of Zinc Oxide Nanoparticles Using Leaf Extract of Sambucus ebulus. *Appl. Sci.* **2020**, *10*, 3620. [CrossRef]
13. Ginting, B.; Maulana, I.; Karnila, I. Biosynthesis Copper Nanoparticles using Blumea balsamifera Leaf Extracts: Characterization of its Antioxidant and Cytotoxicity Activities. *Surf. Interfaces* **2020**, *21*, 100799. [CrossRef]
14. Kieliszek, M.; Bano, I.; Zare, H. A Comprehensive Review on Selenium and Its Effects on Human Health and Distribution in Middle Eastern Countries. *Biol. Trace Element Res.* **2021**, *200*, 971–987. [CrossRef]
15. de Souza, D.F.; da Silva, M.D.C.S.; de Paula Alves, M.; Fuentes, D.P.; Porto, L.E.O.; de Oliveira, P.V.; Kasuya, M.C.M.; Eller, M.R. By-Products as Substrates for Production of Selenium-Enriched *Pleurotus ostreatus* Mushrooms. *Waste Biomass Valoriz.* **2021**, *13*, 989–1001. [CrossRef]
16. Zhang, J.; Wang, H.; Yan, X.; Zhang, L. Comparison of short-term toxicity between Nano-Se and selenite in mice. *Life Sci.* **2005**, *76*, 1099–1109. [CrossRef]
17. Webster, T.J.; Tran, P. Selenium nanoparticles inhibit *Staphylococcus aureus* growth. *Int. J. Nanomed.* **2011**, *6*, 1553–1558. [CrossRef]
18. Chen, T.; Wong, Y.-S.; Zheng, W.; Bai, Y.; Huang, L. Selenium nanoparticles fabricated in Undaria pinnatifida polysaccharide solutions induce mitochondria-mediated apoptosis in A375 human melanoma cells. *Coll. Surf. B Biointerfaces* **2008**, *67*, 26–31. [CrossRef]
19. Ramamurthy, C.; Sampath, K.S.; Arunkumar, P.; Kumar, M.S.; Sujatha, V.; Premkumar, K.; Thirunavukkarasu, C. Green synthesis and characterization of selenium nanoparticles and its augmented cytotoxicity with doxorubicin on cancer cells. *Bioprocess Biosyst. Eng.* **2013**, *36*, 1131–1139. [CrossRef]
20. Wang, H.; Zhang, J.; Yu, H. Elemental selenium at nano size possesses lower toxicity without compromising the fundamental effect on selenoenzymes: Comparison with selenomethionine in mice. *Free Radic. Biol. Med.* **2007**, *42*, 1524–1533. [CrossRef]
21. Vahidi, H.; Barabadi, H.; Saravanan, M. Emerging Selenium Nanoparticles to Combat Cancer: A Systematic Review. *J. Clust. Sci.* **2019**, *31*, 301–309. [CrossRef]
22. Tran, P.A.; Sarin, L.; Hurt, R.H.; Webster, T.J. Opportunities for nanotechnology-enabled bioactive bone implants. *J. Mater. Chem.* **2009**, *19*, 2653–2659. [CrossRef]
23. Bao, P.; Chen, Z.; Tai, R.-Z.; Shen, H.-M.; Martin, F.L.; Zhu, Y.-G. Selenite-Induced Toxicity in Cancer Cells Is Mediated by Metabolic Generation of Endogenous Selenium Nanoparticles. *J. Proteome Res.* **2015**, *14*, 1127–1136. [CrossRef]
24. Khalid, A.; Tran, P.A.; Norello, R.; Simpson, D.A.; O'Connor, A.J.; Tomljenovic-Hanic, S. Intrinsic fluorescence of selenium nanoparticles for cellular imaging applications. *Nanoscale* **2016**, *8*, 3376–3385. [CrossRef]
25. Luo, C.; Xu, Y.; Zhu, Y.; Liu, Y.; Zheng, S.; Liu, Y.; Langrock, A.; Wang, C. Selenium@ Mesoporous Carbon Composite with Superior Lithium and Sodium Storage Capacity. *ACS Nano* **2013**, *7*, 8003–8010. [CrossRef]
26. Chaudhary, S.; Mehta, S.K. Selenium Nanomaterials: Applications in Electronics, Catalysis and Sensors. *J. Nanosci. Nanotechnol.* **2014**, *14*, 1658–1674. [CrossRef]
27. Peng, X.; Wang, L.; Zhang, X.; Gao, B.; Fu, J.; Xiao, S.; Huo, K.; Chu, P.K. Reduced graphene oxide encapsulated selenium nanoparticles for high-power lithium–selenium battery cathode. *J. Power Sources* **2015**, *288*, 214–220. [CrossRef]
28. Ahmed, S.; Brockgreitens, J.; Xu, K.; Abbas, A. Sponge-supported synthesis of colloidal selenium nanospheres. *Nanotechnology* **2016**, *27*, 465601. [CrossRef]
29. Shah, C.P.; Dwivedi, C.; Singh, K.K.; Kumar, M.; Bajaj, P.N. Riley oxidation: A forgotten name reaction for synthesis of selenium nanoparticles. *Mater. Res. Bull.* **2010**, *45*, 1213–1217. [CrossRef]
30. Kamnev, A.A.; Mamchenkova, P.V.; Dyatlova, Y.A.; Tugarova, A.V. FTIR spectroscopic studies of selenite reduction by cells of the rhizobacterium Azospirillum brasilense Sp7 and the formation of selenium nanoparticles. *J. Mol. Struct.* **2017**, *1140*, 106–112. [CrossRef]
31. Quintana, M.; Haro-Poniatowski, E.; Morales, J.; Batina, N. Synthesis of selenium nanoparticles by pulsed laser ablation. *Appl. Surf. Sci.* **2002**, *195*, 175–186. [CrossRef]
32. Ye, X.; Chen, L.; Liu, L.; Bai, Y. Electrochemical synthesis of selenium nanoparticles and formation of sea urchin-like selenium nanoparticles by electrostatic assembly. *Mater. Lett.* **2017**, *196*, 381–384. [CrossRef]
33. Ionin, A.; Ivanova, A.; Khmel'Nitskii, R.; Klevkov, Y.; Kudryashov, S.; Mel'Nik, N.; Nastulyavichus, A.; Rudenko, A.; Saraeva, I.; Smirnov, N.; et al. Milligram-per-second femtosecond laser production of Se nanoparticle inks and ink-jet printing of nanophotonic 2D-patterns. *Appl. Surf. Sci.* **2017**, *436*, 662–669. [CrossRef]
34. Vu, T.T.; Nguyen, D.T.; Nguyen, T.H.; Le, H.T.; Nguyen, D.D.; La, D.D. One-Step Solution Plasma-Mediated Preparation of Se Nanoplarticles and Evaluating Their Acute Oral Toxicity in Mice. *Sustainability* **2022**, *14*, 10294. [CrossRef]
35. Alagesan, V.; Venugopal, S. Green Synthesis of Selenium Nanoparticle Using Leaves Extract of *Withania somnifera* and Its Biological Applications and Photocatalytic Activities. *BioNanoScience* **2018**, *9*, 105–116. [CrossRef]
36. Kokila, K.; Elavarasan, N.; Sujatha, V. Diospyros montana leaf extract-mediated synthesis of selenium nanoparticles and their biological applications. *New J. Chem.* **2017**, *41*, 7481–7490. [CrossRef]
37. Fardsadegh, B.; Jafarizadeh-Malmiri, H. Aloe vera leaf extract mediated green synthesis of selenium nanoparticles and assessment of their In vitro antimicrobial activity against spoilage fungi and pathogenic bacteria strains. *Green Process. Synth.* **2019**, *8*, 399–407. [CrossRef]

38. Sheikhlou, K.; Allahyari, S.; Sabouri, S.; Najian, Y.; Jafarizadeh-Malmiri, H. Walnut leaf extract-based green synthesis of selenium nanoparticles via microwave irradiation and their characteristics assessment. *Open Agric.* **2020**, *5*, 227–235. [CrossRef]
39. Anu, K.; Devanesan, S.; Prasanth, R.; Al Salhi, M.S.; Ajithkumar, S.; Singaravelu, G. Biogenesis of selenium nanoparticles and their anti-leukemia activity. *J. King Saud Univ. Sci.* **2020**, *32*, 2520–2526. [CrossRef]
40. Kalishwaralal, K.; Jeyabharathi, S.; Sundar, K.; Muthukumaran, A. A novel one-pot green synthesis of selenium nanoparticles and evaluation of its toxicity in zebrafish embryos. *Artif. Cells Nanomed. Biotechnol.* **2014**, *44*, 471–477. [CrossRef]
41. Fardsadegh, B.; Vaghari, H.; Mohammad-Jafari, R.; Najian, Y.; Jafarizadeh-Malmiri, H. Biosynthesis, characterization and antimicrobial activities assessment of fabricated selenium nanoparticles using *Pelargonium zonale* leaf extract. *Green Process. Synth.* **2018**, *8*, 191–198. [CrossRef]
42. Pyrzynska, K.; Sentkowska, A. Biosynthesis of selenium nanoparticles using plant extracts. *J. Nanostruct. Chem.* **2021**, *12*, 467–480. [CrossRef]
43. Korde, P.; Ghotekar, S.; Pagar, T.; Pansambal, S.; Oza, R.; Mane, D. Plant extract assisted eco-benevolent synthesis of selenium nanoparticles-a review on plant parts involved, characterization and their recent applications. *J. Chem. Rev.* **2020**, *2*, 157–168.
44. Srivastava, N.; Mukhopadhyay, M. Green synthesis and structural characterization of selenium nanoparticles and assessment of their antimicrobial property. *Bioprocess Biosyst. Eng.* **2015**, *38*, 1723–1730. [CrossRef]
45. Salem, S.S.; Fouda, M.M.G.; Fouda, A.; Awad, M.A.; Al-Olayan, E.M.; Allam, A.A.; Shaheen, T.I. Antibacterial, Cytotoxicity and Larvicidal Activity of Green Synthesized Selenium Nanoparticles Using *Penicillium corylophilum*. *J. Clust. Sci.* **2020**, *32*, 351–361. [CrossRef]
46. Yang, F.; Tang, Q.; Zhong, X.; Bai, Y.; Chen, T.; Zhang, Y.; Li, Y.; Zheng, W. Surface decoration by Spirulina polysaccharide enhances the cellular uptake and anticancer efficacy of selenium nanoparticles. *Int. J. Nanomed.* **2012**, *7*, 835–844. [CrossRef]
47. Nguyen, T.H.; Hoang, N.H.; Van Tran, C.; Nguyen, P.; Dang, T.-D.; Chung, W.J.; Chang, S.W.; Nguyen, D.D.; Kumar, P.S.; La, D.D. Green synthesis of a photocatalyst Ag/TiO_2 nanocomposite using *Cleistocalyx operculatus* leaf extract for degradation of organic dyes. *Chemosphere* **2022**, *306*, 135474. [CrossRef]
48. Thi, H.P.N.; Thi, K.T.P.; Thi, L.N.; Nguyen, T.T.; Nguyen, P.T.; Vu, T.T.; Le, H.T.; Dang, T.-D.; Huynh, D.C.; Mai, H.T.; et al. Green synthesis of an Ag nanoparticle-decorated graphene nanoplatelet nanocomposite by using *Cleistocalyx operculatus* leaf extract for antibacterial applications. *Nano-Struct. Nano-Obj.* **2021**, *29*, 100810. [CrossRef]
49. Shakibaie, M.; Shahverdi, A.R.; Faramarzi, M.A.; Hassanzadeh, G.R.; Rahimi, H.R.; Sabzevari, O. Acute and subacute toxicity of novel biogenic selenium nanoparticles in mice. *Pharm. Biol.* **2012**, *51*, 58–63. [CrossRef]